

Noncollinear magnetism of Cr and Mn monolayers on Cu(111)

Ph. Kurz, G. Bihlmayer, and S. Blügel^{a)}

Institut für Festkörperforschung, Forschungszentrum Jülich, D-52425 Jülich, Germany

Cr and Mn monolayers on a triangular lattice are prototypical examples of frustrated spin systems in two dimensions. Collinear and noncollinear magnetic structures of these monolayers on Cu(111) substrate are investigated on the basis of first-principles total-energy calculations using the full-potential linearized augmented plane-wave method extended by the vector spin-density description for the interstitial and vacuum region. The search for the magnetic minimum-energy configurations included unit cells with one, two, and three atoms. For Cr the minimal energy was found for a 120° spin configuration in a $(\sqrt{3} \times \sqrt{3})R30^\circ$ unit cell, which is in agreement with the classical nearest-neighbor Heisenberg model with antiferromagnetic exchange interaction. The same behavior is expected for Mn, but a surprising result was found: the minimal energy was found for a collinear row-wise antiferromagnetic structure. © 2000 American Institute of Physics.

[S0021-8979(00)51008-1]

I. INTRODUCTION

In the past ultrathin $3d$ transition-metal films grown on oriented single-crystal noble-metal substrates attracted much attention as they exhibit itinerant magnetism and are thus physical realizations of two-dimensional magnetic models. Most experimental and theoretical work focused on overlayers on (001) substrates. The theoretical studies¹ have predicted greatly enhanced magnetic moments in the overlayer and even more important two competing magnetic phases in the monolayer: the $c(2 \times 2)$ antiferromagnetic structure for V, Cr, and Mn monolayers and the $p(1 \times 1)$ ferromagnetic structure for Fe, Co, and Ni monolayers. As results of this investigation we can conclude that the magnetic in-plane nearest-neighbor (n.n.) exchange interaction of V, Cr, and Mn is antiferromagnetic.

Antiferromagnetic interactions on a triangular lattice are the origin of frustrated spin systems. A triangular lattice is provided for example by (111) oriented substrates or by a pseudohexagonal growth of $c(8 \times 2)$ Mn on Cu(100).² The classical n.n. Heisenberg model predicts a noncollinear ground state for the triangular lattice. This configuration has three atoms in a $(\sqrt{3} \times \sqrt{3})R30^\circ$ unit cell. The magnetic moments of the three atoms are aligned at $\pm 120^\circ$.

The aim of this paper is to investigate the ground-state spin structure of Cr and Mn monolayers beyond the Heisenberg model by performing *ab initio* calculations based on the density functional theory. Since the noncollinear calculations are more time consuming than collinear ones we have first applied our theory to unsupported (free standing) monolayers (UML) of Cr and Mn. The UML represents a model system for monolayers (ML) on a noble metal substrate, because the hybridization with the noble metal is very small. Performing the same investigations with a Ag substrate leads to very similar results, which are, however, not presented here.

II. METHOD

The calculation are carried out with the full-potential linearized augmented plane-wave (FLAPW) method in film geometry³ as implemented in the program FLEUR. We are studying the interatomic noncollinear magnetism of $3d$ metals in an environment with low symmetry and open structures. The intraatomic noncollinearity of these systems is small. Therefore, we implemented the noncollinear magnetism as compromise between the interatomic noncollinear treatment of Sandratskii (cf. Ref. 4 and references therein), which relies on the atomic sphere approximation of the magnetization density and direction, and the treatment of the magnetization density as a continuous vector quantity by Nordström *et al.*,⁵ which permitted for the first time the calculation of the intraatomic noncollinearity.

In the density function theory (DFT)⁶⁻⁸ it has been shown that all ground-state properties of a magnetic electron system are uniquely determined by the electron charge-density $n(\mathbf{r})$ and the vector magnetization-density $\mathbf{m}(\mathbf{r})$. In case of a standard collinear treatment of the magnetism, the vector magnetization-density $\mathbf{m}(\mathbf{r})$ reduces to a scalar density $m(\mathbf{r})$. In the FLAPW method in film geometry, the unit cell is partitioned into the muffin-tin spheres, the interstitial and vacuum region, schematically shown in Fig. 1. Within the muffin-tin spheres we include the magnetization density

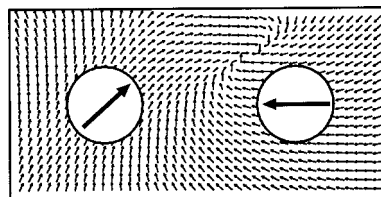


FIG. 1. The magnetization density is treated as vector field in the vacuum and interstitial region within the present “hybrid” implementation of the noncollinear magnetism. Inside each muffin tin the atomic sphere approximation for the magnetization is applied.

^{a)}Electronic mail: s.bluegel@fz-juelich.de

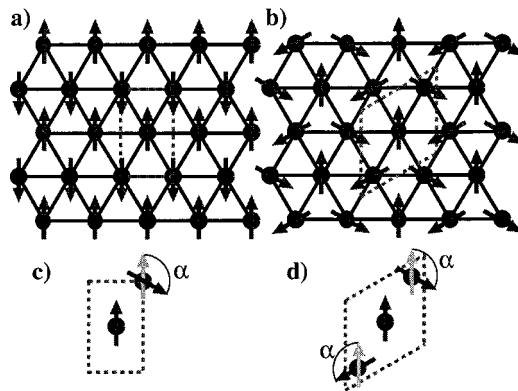


FIG. 2. (a) The row-wise antiferromagnetic structure; (b) the noncollinear 120° configuration. The ferromagnetic structure can be transformed by a continuous rotation into structure (a) as indicated in (c) and into structure (b) as indicated in (d).

without shape approximation, but approximate the magnetization direction by a spherical average, i.e., around each atom there is a local spin-quantization axis and no deviation of the magnetization from this axis is allowed. In the interstitial and vacuum region we include the full continuous vector magnetization density without any shape approximation.

III. COMPUTATIONAL DETAILS

The UMLs have been setup using the geometry and the theoretical lattice constant, $a_0 = 6.65$ a.u., of the Cu(111) surface. The calculations are based on the local spin density approximation (LSDA) of von Barth and Hedin,⁸ but with parameters as chosen by Moruzzi, Janak, and Williams.⁹ About 70 basis functions per atom have been used for all UMLs.

The following different magnetic structures are compared: (i) The ferromagnetic $p(1 \times 1)$ structure; (ii) the row-wise antiferromagnetic structure as shown in Fig. 2(a). The unit cell of this configuration contains two atoms [cf. Fig. 2(c)]. The ferromagnetic structure and the antiferromagnetic structure is connected by a continuous rotation as indicated in Fig. 2(c). (iii) The 120° configuration, which the n.n. Heisenberg model predicts to be energetically preferable for antiferromagnetic materials. The corresponding $(\sqrt{3} \times \sqrt{3})R30^\circ$ unit cell is shown in Fig. 2(d). It is again possible to go from the ferromagnetic structure to the 120° configuration by a continuous rotation, rotating two atoms by the same angle α but in opposite direction, as indicated in Fig. 2(d). If this rotation is continued up to $\alpha = 180^\circ$, the system arrives at an additional collinear antiferromagnetic structure, which will be denoted as the 180° configuration. A k_{\parallel} -point set that corresponds to 180 k_{\parallel} -points in the full two-dimensional Brillouin zone has been used for the unit cell containing two atoms, while the k_{\parallel} -point set for the $(\sqrt{3} \times \sqrt{3})R30^\circ$ unit cell corresponds to 121 k_{\parallel} -points in the full Brillouin zone. It has been checked very carefully that the total energy differences calculated in the two different unit cells are comparable (in particular with respect to the k_{\parallel} -point convergence), by comparing the energy difference between the nonmagnetic and ferromagnetic configuration in both unit cells.

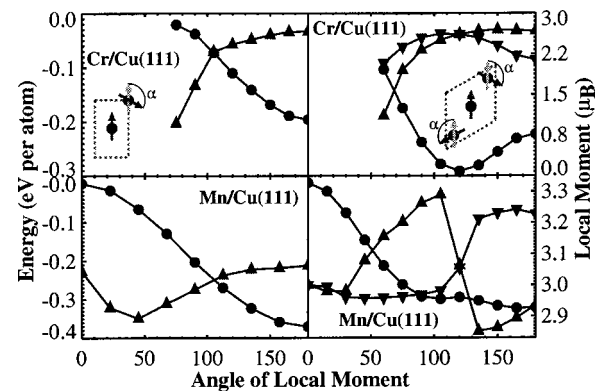


FIG. 3. Calculated energy (filled circles) and magnetic moments (filled triangles) as function of the rotation angle of the local moment for the UML of Cr (upper panels) and Mn (lower images) with the Cu(111) geometry. Generally, the moments of the center atom (triangles pointing upwards) and the outer atoms (triangles pointing downwards) differ in the unit cell with three atoms.

IV. RESULTS

The results of the calculations are presented in Fig. 3. The plots show the total energy (circles) and the magnetic moments (up- and downtriangles) as a function of the rotation angle α . The left-hand side images show rotations that transform the ferromagnetic structure into the row-wise antiferromagnetic structure. The right-hand side show the rotations according to Fig. 2(d). The scales of the left- and right-hand side images are equal, they differ, however, between Cr (upper images) and Mn (lower images).

Consider first Cr: Starting from the row-wise antiferromagnetic solution (Fig. 3 upper-left image) and rotating towards the ferromagnetic structure the magnetic moment decreases rapidly and finally disappears at $\alpha \approx 60^\circ$. Thus, a ferromagnetic solution of the Cr(111) UML in the lattice constant of Cu does not exist. Although the moment changes drastically, the energy shows a cosine-like behavior in the region where a magnetic solution exists, as the n.n. Heisenberg model predicts for an antiferromagnet. The total energy along the rotation path in the unit cell Fig. 2(d) (Fig. 3 upper-right-hand side image) reveals a pronounced minimum at 120° . This minimum and shape of the energy curve matches very well the expectation from the Heisenberg model, although again the moments vanish at $\alpha \approx 60^\circ$, when the system is rotated towards the ferromagnetic state. It is clearly visible that the 120° configuration is the lowest energy configuration among all configurations studied here. Thus, it is the magnetic ground state of the Cr UML predicted by the present investigation.

Now turning to Mn and comparing the results in the two-atom unit-cell (Fig. 3 lower-left-hand side image) with those of Cr (Fig. 3, upper-left-hand side image) we find the behavior of Mn and Cr is very similar, i.e., the energy curve is cosine-like and Mn prefers to be antiferromagnetic. However, in contrast to Cr the ferromagnetic state exists and the magnetic moments change only within a narrow range, $2.9\mu_B - 3.05\mu_B$, with the rotation. The lower-right-hand-side image reveals a surprise. The total energy of the Mn system with three atoms per unit cell does not exhibit a mini-

mum at 120° , as commonly expected by the simple Heisenberg model. In fact, the energy curve is almost flat between 100° and 180° . Apparently, the 180° configuration is even lower in energy than the 120° configuration. In summary, the lowest energy configuration among all magnetic structures investigated, is the row-wise antiferromagnetic configuration.

V. CONCLUSION

We have implemented the noncollinear magnetism into the FLAPW program FLEUR in terms of a vector spin-density formalism in the interstitial and vacuum region and the muffin-tin averaged magnetization direction. We have applied this method to investigate the magnetic interaction of Cr and Mn(111) UML with the Cu lattice constant and a Mn monolayer on Cu(111). We investigated the minimum-energy magnetic configuration by calculating the total energy for different spin structures. The search included magnetic configurations with one, two, and three atoms per unit cell and continuous paths of noncollinear magnetic states between magnetic high symmetry states. We found that Cr behaves to a large extent according to the n.n. Heisenberg model, although the moments do change drastically. The 120° configuration on the triangular lattice has the lowest energy among all configurations investigated. Since it behaves according to the n.n. Heisenberg model we believe this is the magnetic ground state. For Mn we found a surprising result: the 120° configuration on the triangular lattice is not

the lowest energy configuration in contradiction to the Heisenberg model. Instead the row-wise antiferromagnetic state has the lowest energy. At present we cannot rule out whether a more complicated configuration with a lower energy exists. We consider it an experimental challenge to unravel the magnetic structure of these monolayers and to prove or disprove our predictions.

ACKNOWLEDGMENTS

The authors thank Lars Nordström and Leonid Sandratskii for many fruitful discussions during the course of this work. This work was supported by the Deutsche Forschungsgemeinschaft under Grant No. BL444/1-1 and the TMR Networks, Contract Nos. EMRX-CT96-0089 and FMRX-CT98-0178.

¹M. Weinert and S. Blügel, in *Magnetic Multilayers*, edited by L. H. Bennett and R. E. Watson (World Scientific, Singapore, 1993).

²T. Flores, M. Hansen, and M. Wuttig, *Surf. Sci.* **279**, 251 (1992).

³E. Wimmer, H. Krakauer, M. Weinert, and A. J. Freeman, *Phys. Rev. B* **24**, 864 (1981); M. Weinert, E. Wimmer, and A. J. Freeman, *ibid.* **26**, 4571 (1982).

⁴L. M. Sandratskii, *Adv. Phys.* **47**, 91 (1998).

⁵L. Nordström and D. J. Singh, *Phys. Rev. Lett.* **76**, 4420 (1996).

⁶P. Hohenberg and W. Kohn, *Phys. Rev. B* **136**, 846 (1964).

⁷W. Kohn and L. J. Sham, *Phys. Rev. A* **140**, 1133 (1965).

⁸U. von Barth and L. Hedin, *J. Phys. C* **5**, 1629 (1972).

⁹V. L. Moruzzi, J. F. Janak, and A. R. Williams, *Calculated Electronic Properties of Metals* (Pergamon, New York, 1978).